OXADIAZOLE DERIVATIVES AS POTENTIAL EGFR PROTEIN KINASE INHIBITORS: PREDICTION OF IN-SILICO ADMET PROPERTIES AND MOLECULAR DOCKING STUDY

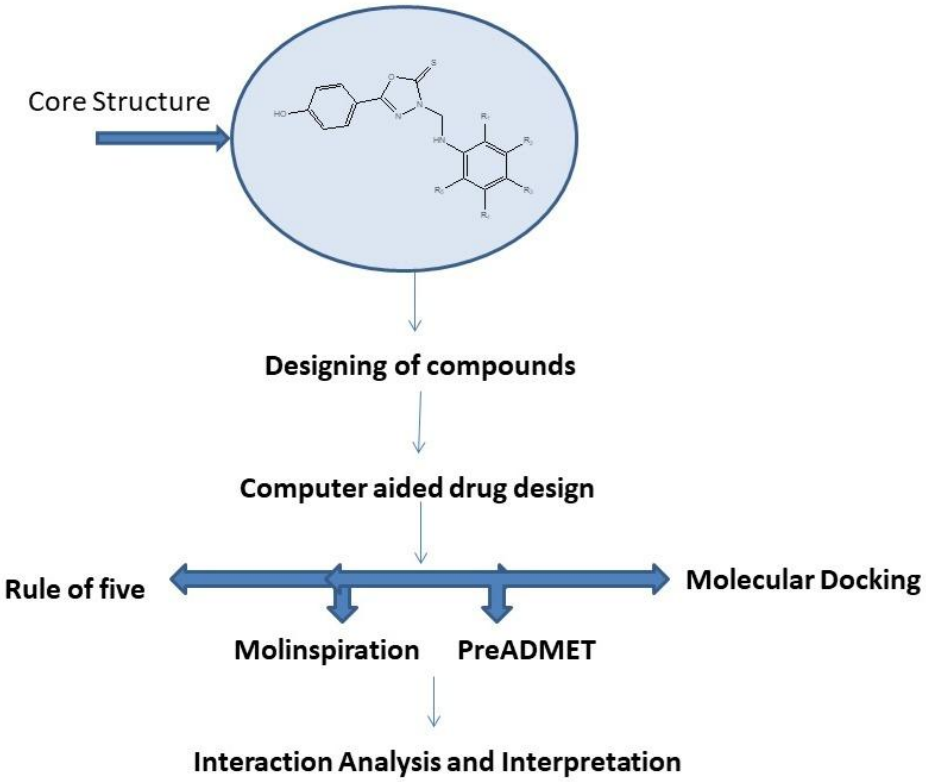

ABSTRACT

Background: Hepatocellular carcinoma is strongly linked to abnormalities in the EGFR triggers pathway, which is crucial for tumor cell growth, survival, and the formation of new blood vessels. This study investigates the potential of targeting EGFR-mediated pathways to inhibit tumor growth and progression, offering insights into the development of novel treatments for HCC. **Methods:** The methodology involves design of a virtual library of 1,3,4-oxadiazole derivatives, performing *in-silico* computational prediction, and conducting ADMET analysis property to evaluate the pharmacokinetic and toxicity profiles of the selected compounds. A molecular docking study was performed using 30

compounds on PDB ID: 1M17 with Molegro Virtual Docker to investigate the binding patterns of ligand molecules at their target site. **Results:** The drug likeness, Molinspiration and preADMET properties of 1,3,4-Oxadiazole designed derivatives have been found to be within the recommended acceptable range. Among all the derivatives, S10 and S23 exhibited the most impressive inhibitory potential against the EGFR receptor. The derivatives were observed with higher docking scores (-127.637 and -148.27) with Re-rank score (−98.405.11 and −117.52 kcal/mol) than the Co-crystallized ligand (Docking score -124.917; Re-rank score -93.688 kcal/mol). Compound S23 showing 4 H-bond interactions i.e. Met 769, Gln767, Thr766, Asp831 which is significant as compared to standard drug Afatinib having dock score of -134.695 and with 1 H-bond interactions i.e. Lys 721 Docking results proposed that these newly designed compounds might be used as EGFR inhibitors. **Conclusion:** This systematic screening provides a robust foundation for selecting and refining molecules with the best potential for therapeutic application, aligning with both scientific innovation and regulatory compliance.

KEYWORDS

1,3,4-oxadiazole, Hepatocellular carcinoma, Liver Cancer, EGFR, *in-silico* study.

INTRODUCTION

Oxadiazole is a five-membered heterocyclic ring containing oxygen, sulfur and nitrogen atoms. It displays aromaticity due to the extended delocalization of π-electrons within the ring system. It is widely studied due to their diverse applications in medicinal chemistry, agriculture, and materials science. Among all isomers of oxadiazole 1,3,4-oxadiazole isomer is the most studied and stable isomer [1,2]. The 1,3,4-oxadiazole demonstrates anticancer properties driven by its aromatic structure and the ability to interact with key biological targets like DNA, RNA, and proteins. These interactions disrupt cancer cell functions, leading to potential anticancer effects [3,4].

Hepatocellular carcinoma (HCC) is a form of liver cancer that develops in an organ essential for metabolism, detoxification, and nutrient regulation.

HCC is a worsening worldwide health challenge, with growing prevalence linked to risk factors such as chronic liver disease, viral infections and alcoholic disease. It is among the leading causes of cancer-related mortality worldwide [5,6]. The burden of cancer is expected to increase to 20.3 million by 2026 and 23.6 milliion by 2030 [7,8].

In liver cell the most frequent process that happens during the cell cycle is protein phosphorylation. Different types of specialised kinases and phosphates that can add or remove phosphates regulate phosphorylation. The kinase's involves in biological process, including signal transduction, regulation, proliferation, death. Kinase's main function is to catalyze the process by which ATP's gama-phosphate group is transferred to the substrate. The location of kinase receptors, which sustain internal and external communication, is critical for the cell shape. EGFR is a tyrosine kinase enzyme that drives cancer development by enhancing cell proliferation, blocking apoptosis, supporting metastasis, and stimulating blood vessel formation. This phosphorylation triggers a series of intracellular signaling pathways, including:

- **RAF/RAS/ERK/MEK pathway:** Regulates cell growth, proliferation, and differentiation.
- **AKT/PI3K/mTOR pathway:** Modulates cell viability and biochemical function.
- **JAK/STAT pathway:** Implicated in immune response and cellular growth.

Under normal conditions, this process is tightly regulated. However, mutations or overexpression of EGFR can lead to unchecked activation of these pathways, promoting oncogenesis [9,10,11,12].

Erlotinib, gefitinib, and cetuximab, have been investigated for their potential in treating HCC. Erlotinib and gefitinib, as small-molecule tyrosine kinase inhibitors, block the phosphorylation of EGFR, disrupting downstream signaling pathways involved in cell proliferation and survival. Cetuximab, a monoclonal antibody, binds to the outer domain of EGFR, inhibiting ligand-driven activation. Though their effectiveness in HCC is still under investigation, these drugs, especially in combination with sorafenib or immune checkpoint inhibitors hold potential for improving treatment results in EGFR-positive liver cancer [13].

The objective of this Work is to develop and optimise novel inhibitors that target the well-known oncology therapeutic target, EGFR protein kinase. Make sure the compounds have good pharmacokinetic and safety profiles that are appropriate for oral bioavailability and therapeutic

development, analyse the molecular interactions between the proposed inhibitors, optimise compound activity, and assess ADMET profiles.

MATERIALS AND METHODS

Designing of ligand

A virtual library comprising 30 newly designed 1,3,4-oxadiazole ligands. The structure of derivative ligands are examined **Figure 1**. These compounds feature a variety of functional groups with differing polarities, including amino, acetyl, methyl, hydroxyl, nitro, and halogen groups. The ligands were draw using ChemDraw Ultra 2D 8.0 software, and Chem3D Ultra 8.0 software for molecular modeling, energy minimization using molecular mechanics, enables calculation of molecular geometries, bond angles, and distances and saved in .mol, .pdb formats for further computational studies. Their novelty was validated through searches in chemical databases such as PubChem and Zinc 20 [14,15,16].

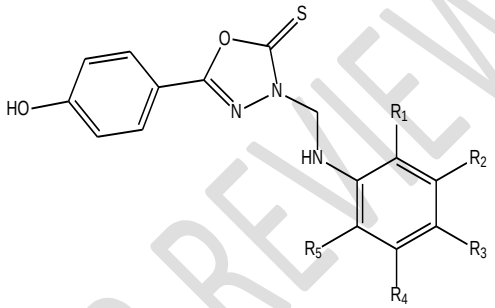

Figure 1: 1,3,4-Oxadiazole derivatives with substitutions

Determination of Molecular Properties

Drug-likeness evaluation based on Lipinski's criteria

RO5 helps predict oral bioavailability, stating that a drug-like molecule should have limited hydrogen bond donors and acceptors, a molecular weight under 500 daltons, and a logP below 5 for optimal solubility and permeability.

The calculations were performed using an online server **(http://www.scfbio-iitd.res.in/software/drugdesign/lipinski.jsp)** [17, 18].

Molinspiration-based drug-likeness and biological activity prediction

Molinspiration provides a wide range of cheminformatics software tools for processing and manipulating molecules. It is a free web based tool for the determination of physicochemical features such as logP, molecular weight, TPSA, hydrogen bond donors/acceptors and prediction of bioactivity. Determination of bioactivity in molinspiration is based on byasian algorithm model. It is fragment based model which contains some numerical values of fragments and sum of these numerical values of

fragments gives the prediction of bioactivity score when compared to standard. These tools include those for converting between SMILES and .mol files, normalising molecules, creating tautomers, fragmenting molecules, calculating various molecular properties required for QSAR, and molecular modelling. https://www.molinspiration.com/ online Molinspiration software is used for study [19, 20, 21].

PreADMET Analysis

Pre-ADMET studies play a pivotal role in during the initial phases of drug discovery and development, enabling to evaluate potential drug candidates for their pharmacokinetic, safety, efficacy and toxicity profiles before advancing to costly in vivo experiments or clinical trials. By predicting factors like intestinal permeability, plasma protein binding, metabolic stability, and potential toxicity (e.g., hepatotoxicity or hERG channel inhibition), pre-ADMET analyses help optimize lead compounds, reduce the likelihood of late-stage failures, and streamline the drug development pipeline. preADMET software utilizing an online server **(**https://preadmet.webservice.bmdrc.org/) for calculations [22, 23].

Docking Study

A molecular docking study was performed using Molegro Virtual Docker (MVD 6.0) to analyze the binding patterns of 30 compounds on PDB ID: 1M17, utilizing a 64-bit Windows 7 system powered by a Lenovo Intel Core i3 12th Gen processor. 10 compounds were selected on the basis of good docking score and their interaction with the receptor. The X-ray crystallography structures of EGFR Tyrosine kinase enzyme, chemical name- [6,7-bis(2-methoxy-ethoxy)uinazoline-4-yl]-(3-ethynylphenyl)amine was retrieved from RCSB protein data bank [24]. Reported Amino Acid Interaction of PDB: 1M17 are Met769, Gly839 Amino acid residue, and Thr766, Lys721, Leu764, Asp831, Cys751, Lys828, Arg752, Glu738 Neigh bouring residue.

Validation of Docking Methodology

A vital step of validation of docking is ensuring the accuracy of the docking approach. This was achieved through redocking, in which the natural co-crystallized ligand was reintroduced into the binding site from the PDB and utilized to verify the program's correctness. The validation study shown RMSD value for the dock orientation was found to be 1.78, which is lower than the crystal resolution of the 1M17 protein structures ($2.60A^0$) reported in the protein data bank **Figure 2**. Additionally, the docked ligand displayed a hydrogen bond and a hydrophobic contact with nearly the same amino acid atoms as the native co-crystallized ligand, and the hydrogen bond length was similarly discovered to be smaller than 3.9 A^0.

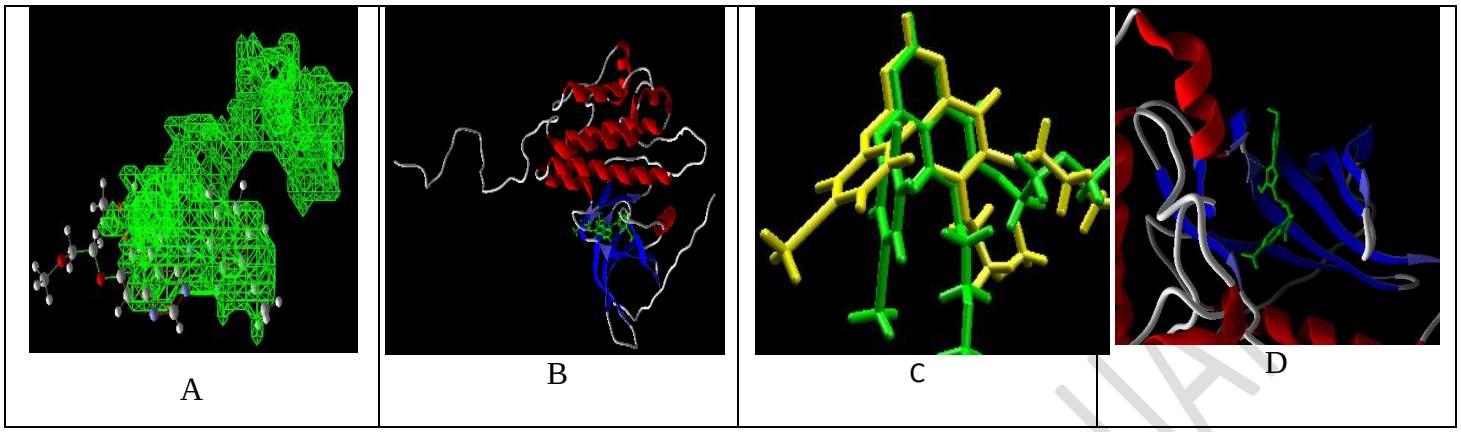

Figure 2: A: Active site prediction, B: Ligand preparation C: Validation of docking procedure for 1M17 Protein: Binding orientation of native co-crystallized ligand (green colour) and docked pose of ligand (Yellow colour), D: Docking View of Compound S23

RESULTS

The Lipinski's rule of five properties of 1,3,4-Oxadiazole have been found to be within the acceptable range. The molecular weight being less than 500 Daltons falls within the acceptable range for drug-likeness. Additionally, hydrogen bond donor, hydrogen bond acceptor, and logP properties follow the RO5 **Table 1**. The Molinspiration analysis provided key parameter values critical for assessing the compound's potential. The LogP value ranging from 2 to 3.9 indicates that all the derivatives possess moderate to high lipophilicity, which favors membrane permeability. The TPSA, calculated as <110Å^2, suggests the compound is likely to exhibit favorable absorption and solubility characteristics. The bioactivity scores include 0.77 for kinase inhibition, indicating promising activity in enzyme targeting, and -0.70 for GPCR ligand activity, suggesting moderate interaction potential with G-protein-coupled receptors. 0 rotation bond value indicated that derivatives have flexibility **Table 2, 3.** These parameter values collectively provide a comprehensive understanding of the optimization of its drug-likeness and therapeutic potential, aiding in the development of more effective and safer therapeutic agents.

DISCUSSION

PreADMET discussion

The PreADMET results were analyzed to evaluate the pharmacokinetic properties and toxicity profiles of the selected compounds. These results provide a comprehensive understanding of the ADMET properties along with properties under Five; drug-likeness. The 1,3,4-Oxadiazole derivative have high bioavailability along with good solubility and cellular permeability, low BBB permeability, high predicted intestinal absorption, and potential for cytochrome P450 enzyme inhibition. Additionally, toxicity assessments, including non-mutagenicity, carcinogenicity, and acute toxicity, were examined to

predict the safety profile of the compounds **Table 4.** The findings serve as a critical step in identifying promising candidates for subsequent In-vitro and In-vivo studies, ensuring to development of safer and more efficacious therapeutic agents. The compounds S1, S3, S9, S10, S11, S15, S18, S23, S27, and S28 successfully pass the in-silico computational prediction screening, demonstrating good ADMET properties along with favorable pharmacokinetic and toxicity profiles.

Table 1: Results of Lipinski's rule of five calculations

S. No	Compound Code	Mass	HBD	HBA	LOGP	Molar Refractivity
1.	S1	299.00	2	4	3.28	84.25
2.	S2	344.00	2	6	3.19	90.91
3.	S3	344.00	2	6	3.19	90.91
4.	S4	344.00	2	6	3.19	90.91
5.	S5	333.50	2	4	3.16	86.33
6.	S6	333.50	2	4	3.16	86.33
7.	S7	333.50	2	4	3.16	86.33
8.	S8	343.00	3	6	2.98	91.21
9.	S9	343.00	3	6	2.98	91.21
10.	S10	315.00	2	5	2.99	85.92
11.	S11	315.00	2	5	2.99	85.92
12.	S12	313.00	2	4	3.59	88.99
13.	S13	313.00	2	4	3.59	88.99
14.	S14	377.00	2	6	3.54	95.73
15.	S15	341.00	1	6	2.68	94.63
16.	S16	403.00	1	5	4.52	93.88
17.	S17	279.00	2	4	2.56	77.10
18.	S18	300.00	2	5	2.68	82.05
19.	S19	325.00	1	5	2.46	87.11
20.	S20	299.50	2	5	1.27	70.19
21.	S21	342.00	3	6	2.11	91.23
22.	S22	314.00	3	5	2.79	87.39
23.	S23	404.00	3	9	2.60	100.70
24.	S24	251.00	1	4	1.73	67.87
25.	S25	279.00	1	5	1.97	77.95
26.	S26	375.00	1	5	4.46	110.05
27.	S27	378.00	4	7	3.01	95.67
28.	S28	266.00	4	6	0.84	66.91

29.	S29	352.00	5	8	0.48	87.17
30.	S30	333.50	2	4	3.16	86.33

168

169 **Table 2: Result of Molecular Properties using online program (Molinspiration)**

S. No	CODE	Molecular Properties								
		miLogP	TPSA	n atoms	MW	nON	nOHNH	NV	NR	Volume
1	S1	2.65	63.22	21	299.36	5	2	0	4	254.72
2	S2	2.57	109.0	24	344.35	8	2	0	5	278.06
3	S3	2.61	109.0	24	344.35	8	2	0	5	278.06
4	S4	2.58	109.0	23	330.32	8	2	0	4	261.25
5	S5	3.29	63.22	22	333.80	5	2	0	4	268.26
6	S6	3.31	63.22	22	333.80	5	2	0	4	268.26
7	S7	3.33	63.22	22	333.80	5	2	0	4	268.26
8	S8	2.54	100.5	24	343.36	7	3	0	5	281.72
9	S9	2.57	100.5	24	343.36	7	3	0	5	281.72
10	S10	2.39	83.45	22	315.35	6	3	0	4	262.74
11	S11	2.18	83.45	22	315.35	6	3	0	4	262.74
12	S12	3.06	63.22	22	313.38	5	2	0	4	271.28
13	S13	3.10	63.22	22	313.38	5	2	0	4	271.28
14	S14	2.31	97.36	25	377.45	7	2	0	5	302.71
15	S15	2.26	71.50	24	341.39	6	1	0	4	290.65
16	S16	3.93	71.50	29	403.46	6	1	0	5	345.50
17	S17	2.40	63.22	19	279.37	5	2	0	6	250.28
18	S18	1.76	76.11	21	300.34	6	2	0	4	250.57
19	S19	2.22	81.91	23	325.35	7	1	0	3	263.37
20	S20	0.89	80.29	19	299.74	6	2	0	4	232.63
21	S21	1.75	92.32	24	342.38	7	3	0	5	286.11
22	S22	2.42	75.25	22	314.37	6	3	0	5	267.12
23	S23	2.26	106.9	28	404.36	9	3	0	7	213.79
24	S24	1.20	54.43	17	251.31	5	1	0	3	216.82
25	S25	1.96	54.43	19	279.37	5	1	0	5	250.42
26	S26	4.60	54.43	27	375.45	5	1	0	5	326.51
27	S27	1.35	123.3	25	378.44	8	4	0	5	297.44

28	S28	0.23	106.3	18	266.28	7	4	0	3	213.59
29	S29	2.53	143.6	24	352.37	9	5	0	7	291.02
30	S30	3.33	63.22	22	333.80	5	2	0	4	268.26

170

171 **Table 3: Result of Bioactivity score of the ligand and its complexes**

S. No	Comp. Code	Molinspiration biological activity					
		GPCR ligand	Ion channel modulator	Kinase inhibitor	Nuclear receptor ligand	Protease inhibitor	Enzyme inhibitor
1	S1	-0.81	-0.77	0.73	-0.85	-1.04	-0.04
2	S2	-0.83	-0.79	-0.81	-0.96	-1.03	-0.14
3	S3	-0.82	-0.72	0.77	-0.79	-0.98	-0.15
4	S4	-0.44	-0.71	-0.46	-0.40	-0.68	-0.11
5	S5	-0.79	-0.75	-0.66	-0.86	-1.07	-0.12
6	S6	-0.76	-0.74	-0.69	-0.81	-1.04	-0.10
7	S7	-0.75	-0.74	-0.75	-0.80	-1.01	-0.08
8	S8	-0.68	-0.72	0.67	-0.57	-0.83	-0.02
9	S9	-0.67	-0.71	0.67	-0.56	-0.82	-0.02
10	S10	-0.76	-0.89	0.69	-0.82	-1.04	-0.06
11	S11	-0.75	-0.73	0.67	-0.77	-0.96	-0.04
12	S12	-0.81	-0.81	-0.72	-0.79	-1.05	-0.12
13	S13	-0.80	-0.82	-0.73	-0.81	-1.03	-0.11
14	S14	-0.54	-0.84	-0.64	-0.62	-0.59	-0.03
15	S15	-0.63	-0.86	0.65	-0.72	-0.80	-0.14
16	S16	-0.50	-0.69	-0.48	-0.55	-0.65	-0.10
17	S17	-0.72	-0.85	-0.84	-0.86	-0.99	0.03
18	S18	-0.58	-0.67	0.43	-0.79	-0.83	0.08
19	S19	-0.53	-0.91	-0.61	-0.58	-0.81	-0.09
20	S20	-1.11	-1.21	-0.95	-1.09	-1.23	-0.23
21	S21	-0.64	-0.96	-0.62	-0.84	-0.76	-0.12
22	S22	-0.76	-0.89	-0.65	-1.11	-0.92	-0.06
23	S23	-0.70	-0.87	0.72	-1.08	-0.88	-0.19
24	S24	-1.07	-1.13	-1.05	-1.27	-1.51	-0.14
25	S25	-0.87	-1.13	-0.88	-1.11	-1.34	-0.08
26	S26	-0.42	-0.60	0.40	-0.44	-0.64	0.03
27	S27	-0.73	-0.74	0.59	-0.89	-0.63	0.09

28	S28	-0.94	-1.08	0.86	-1.15	-1.11	-0.03
29	S29	-0.30	-0.52	-0.60	-0.62	-0.29	0.24
30	S30	-0.75	-0.74	-0.70	-0.80	-1.01	-0.08

172 **Table 4: Result of In-silico ADME properties of designed compounds**

Properties	Range	Features	Compounds
BBB(Blood Brain Barrier)	More than 1	CNS active compounds	S1, S5, S6, S7, S10, S13, S16, S19, S21, S22, S30
	Less than 1	CNS inactive compounds	S2, S3, S4, S8, S9, S11, S12, S14, S15, S17, S18, S20, S23, S24, S25, S26, S27, S28, S29
HIA (Human Intestinal Absorption)	0-20%	Poor absorption	-----
	20-70%	Moderate absorption	S23,S29
	70-100%	Higher absorption	S1, S2, S3, S4, S5, S6, S7, S8, S9, S10, S11, S12, S13, S14, S15, S16, S17, S18, S19, S20, S21, S22, S24, S25, S26, S27, S28, S30
PPB (Plasma Protein Binding)	More than 90%	Strongly bounded	S1, S2, S3, S4, S5, S6, S7, S8, S9, S10, S14, S15, S16, S18, S19, S21, S22, S26, S27
	Less than 90%	Weakly bounded	S11, S12, S13, S17, S20, S23, S24, S25, S28, S29, S30
Caco-2 Permeability	Less than 4	Lower	S14, S27
	4-70	Moderate	S1, S2, S3, S4, S5, S6, S7, S8, S9, S10,S11, S12, S13, S15, S16, S17, S18, S19, S20, S21, S22,S23, S24, S25, S26, S28,S29, S30
	More than 70	Higher	--------
CYP2D6	Non-inhibitor	Acceptance Yes	S1, S2, S3, S4, S5, S6, S7, S8, S9, S10, S11, S12, S13, S14, S15, S16, S17, S18, S19, S20, S21, S22, S23, S26, S27, S28,S29, S30
	Inhibitor	Acceptance No	S24, S25
MDCK (Madin-Darby Canine Kidney)	Less than 25	Lower	S1, S2, S3, S4, S5, S6, S7, S8, S9, S10, S11, S12, S13, S14, S15, S16, S17, S18, S19, S20, S21, S22, S23, S25, S26, S27,S29, S30
	25-500	Moderate	S24, S28
	More than 500	Higher	---------
P-gp_ Inhibition	Non-inhibitor	Acceptance No	S17, S18, S19, S20, S21, S22, S24, S25, S27, S28, S29
	Inhibitor	Acceptance Yes	S1, S2, S3, S4, S5, S6, S7, S8, S9, S10, S11, S12, S13, S14, S15, S16, ,S23, S26, S30

Result of Drug Likeness of synthesized compounds

Drug Likeness		Compounds
CMC_like_ Rule	Qualified	S1, S2,S3, S4, S5, S6, S7, S8, S9, S10, S11,S12, S13, S14, S15, S16, S17, S18, S19, S20, S21, S22, S23, S24, S25, S27, S28, S29, S30
	Not qualified	S26
MDDR_like_ Rule	Mid Structure	S1,S2, S3, S4, S5, S6, S7, S8, S9, S11, S12, S13, S14, S15, S16, S17, S18, S19, S20, S21, S22, S24, S25, S26, S27, S28, S29, S30
	Drug Like	S10, S23
Rule_of_Five	Suitable	S1, S2, S3, S4, S5, S6, S7, S8, S9, S10, S11, S12, S13, S14, S15, S16, S17, S18, S19, S20, S21, S22, S23, S24, S25, S26, S27, S28, S29, S30
	Not Suitable	----------

Result of Toxicity studies of synthesized compounds

Toxicity		Compounds
Ames_test	Mutagen	S2, S4, S5, S6, S7, S8, S12, S13, S14, S16, S17, S19, S20, S21, S22, S24,

		S29, S30
	Non-Mutagen	S1, S3, S9, S10, S11, S15, S18, S23, S25, S26, S27, S28
Carcino_Mouse	Negative	S1, S2,S3, S4, S5, S6, S7, S8, S9, S10, S11, S12, S13, S14, S15, S16, S17, S18, S19, S20, S21, S22, S23, S24, S25, S26, S27, S28, S29, S30
	Positive	--------
Carcino_Rat	Negative	S1, S2, S3, S5, S6, S7, S8, S9, S10, S11, S12, S13, S14, S15, S16, S17, S18, S20, S21, S22, S24, S25, S26, S27, S28, S29, S30
	Positive	S4, S19, S23
hERG_inhibition	Ambiguous	S14, S27, S39
	Medium Risk	S1, S2, S3, S4, S5, S6, S7, S8, S9, S10, S11, S12, S13, S15, S17, S18, S19, S20, S21, S22, S24, S25, S28, S29, S30
	Low-risk	S16, S23, S26

Molecular Docking Discussion:

The strong activity of the target compound, demonstrated by its impressive docking score and binding pattern, is reinforced by its ability to engage key amino acids within the target protein's binding site. The molecular docking studies aligned with the biological test results, highlighting the remarkable inhibitory potential of compounds S10 and S23 against the EGFR was observed with higher docking scores (-127.637 and -148.27) with Re-rank score (−98.405.11 and −117.52 kcal/mol) than the Co-crystallized ligand (Docking score -124.917; Re-rank score -93.688 kcal/mol). Compound S23 showing 4 H-bond interactions i.e. Met 769, Gln767, Thr766, Asp831 which is significant as compared to standard drug Afatinib having dock score of -134.695 and with 1 H-bond interactions i.e. Lys 721 **Fig. 3 & 4.** Docking results proposed that these newly designed compounds might be used as EGFR inhibitors **Table 5**.

	S1	S3	S9
	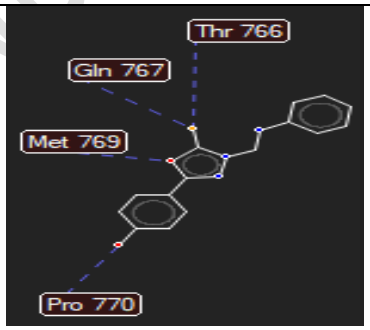	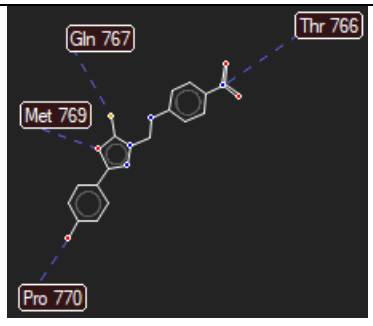	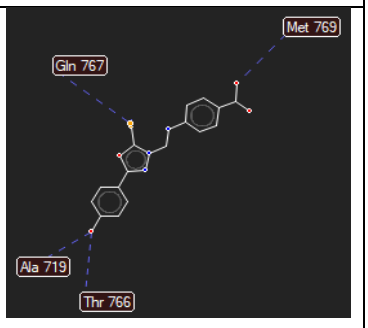

H-Bond Interactions	S10	S11	S15
	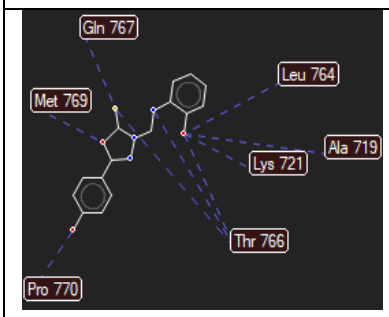	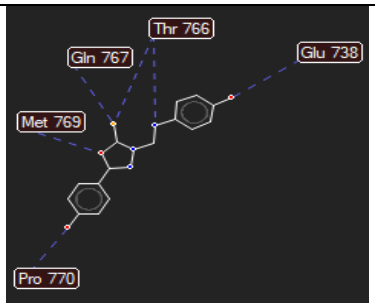	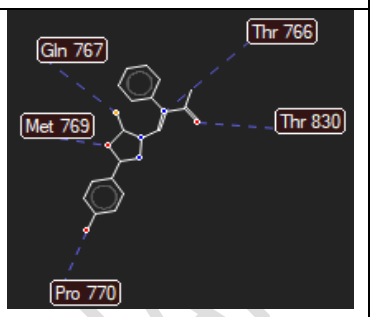
	S18	**S23**	**S27**
	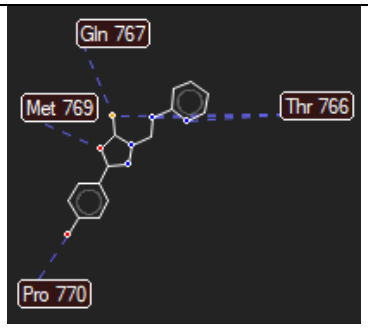	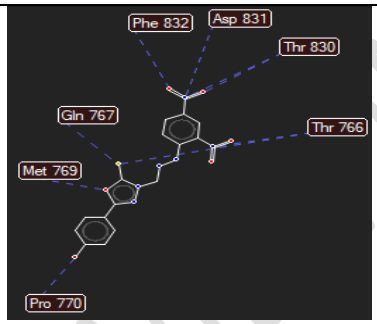	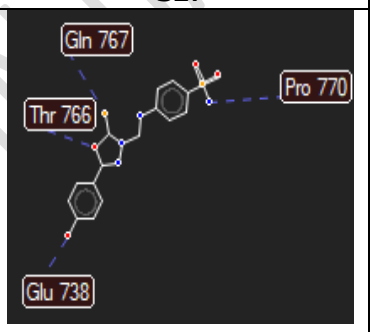
	S28	**Docking Interaction of Co-crystallized ligand**	**AFATINIB**
	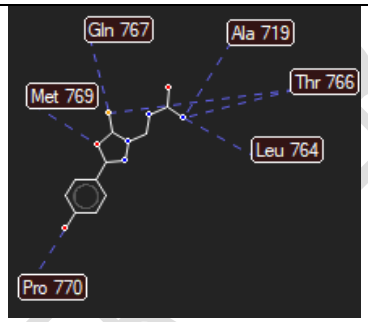	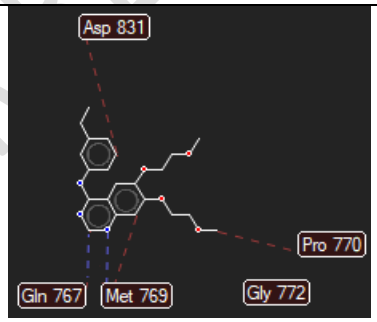	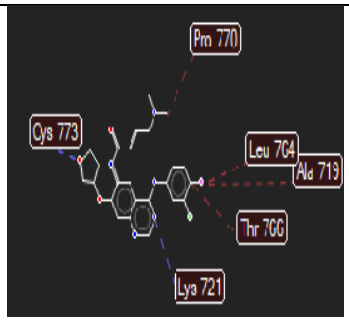

188 **Fig . 3:** Docking Interactions of derivatives, Co-crystallized ligand and standard drug Afatinib on PDB 1M17

189

190 **Table 5: Docking score and interaction of oxadiazole derivatives**

S. N.	Comp.	Docking Score (Kj/mol)			Docking Interaction	
		Mol dock score	Rerank score	H-Bond	H-Bond interactions	Other Interaction
1.	S1	-117.78	-91.600	-7.229	Met 769, Gln767, Thr766	-------
2.	S3	-117.756	-84.884	-6.7136	Met 769, Gln767, Thr766	Leu764
3.	S9	-117.554	-91.207	-5.23676	Met 769, Gln767, Thr766	---------

4.	S10	-127.637	-98.405	-11.4803	Met 769, Gln767, Thr766, Lus721	Leu764
5.	S11	-121.686	-91.630	-10.2563	Met 769, Gln767, Thr766, Glu738	Leu764
6.	S15	-119.082	-81.826	-6.84307	Met 769, Gln767, Thr766	Met769, Lys721, Leu764
7.	S18	-115.508	-88.202	-8.8763	Met 769, Gln767, Thr766	Leu764
8.	S23	-148.271	-117.52	-11.5519	Met 769, Gln767, Thr766, Asp831	-------
9.	S27	-110.52	-87.282	-5.29275	Met 769, Gln767, Thr766, Glu738	Leu764
10.	S28	-104.089	-73.112	-9.54911	Met769, Thr766, Gln767	Lys721. Gln767
11.	Co-crystal	-124.917	-93.688	-1.92232	Met 769, Gln767	----------
12.	Afatinib	-134.695	-107.162	-4.2489	Lys721	Thr766

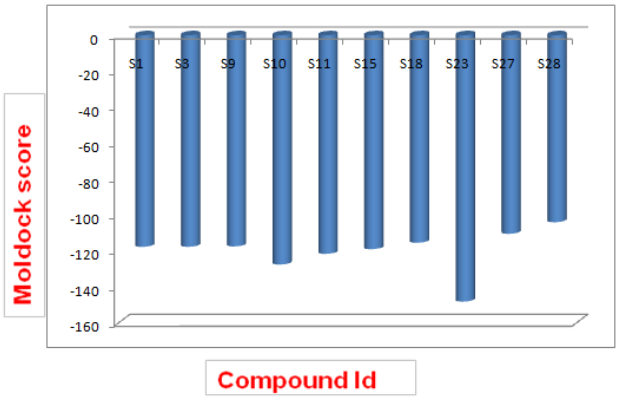

Fig . 4: Statics graph of Docking Interactions scores of derivatives on PDB 1M1

CONCLUSION

The compounds S10 and S23 successfully passed the in-silico computational prediction screening, indicating their robust ADMET profiles, which align well with the requirements for drug-likeness and safety. Their pharmacokinetic parameters suggest efficient bioavailability and systemic distribution, while their toxicity profiles demonstrate minimal risk, making them strong candidates for further experimental validation and development.

ACKNOWLEDGEMENTS

We would like to acknowledge the GRY Institute of Pharmacy, Borawan for providing the research facilities.

CONFLICT OF INTEREST

The authors declare no conflict of interest.

FUNDING SOURCES

NIL

AUTHOR CONTRIBUTION

All authors have approved the final version of the article. All authors take public responsibility for the paper as a whole, i.e., conception and design, data, analysis, interpretation, and approval of the final version of the manuscript.

REFERENCES

1. Patidar Mohini, Mandloi Nilesh, et al. Design, Synthesis and Evaluation of 1, 3, 4-Oxadiazole Derivatives for Antidiabetic Activity. JCHR, 14(2), 1942-1949 (2024)
2. Tariq Javida Muhammad, Rahima Fazal, et al. Synthesis, SAR elucidations and molecular docking study of newly designed isatin based oxadiazole analogs as potent inhibitors of thymidine phosphorylase. Bioorganic Chemistry, 79, 323–333 (2018) https://doi.org/10.1016/j.bioorg.2018.05.011
3. Hayat Ullah, Fazal Rahim, et al. Synthesis, molecular docking study and in vitro thymidine phosphorylase inhibitory potential of oxadiazole derivatives. Bioorganic Chemistry, 78, 58–67 (2018) https://doi.org/10.1016/j.bioorg.2018.02.020
4. Han-Syuan Lin, Yi-Luen Huang, et al. Identification of novel anti-liver cancer small molecules with better therapeutic index than sorafenib via zebrafish drug screening platform. Cancers, 11, 739 (2019) https://doi.org/10.3390/cancers11060739
5. Smith Robert, Kevin C. Oeffinger. The Importance of Cancer Screening. Med Clin N Am, 1, 20 (2020) https://doi.org/10.1016/j.mcna.2020.08.008
6. Mathur Prashant, Sathishkumar Krishnan et al. Cancer Statistics 2020: Report from national cancer registry program India. 6, 1063-1075 (2020) https://doi.org/10.1200/GO.20.00122
7. Cancer National Institute (NIH) https://www.cancer.gov/types
8. Komposch Karin and Sibilia Maria. EGFR Signaling in Liver Diseases. Int. J. Mol. Sci, 17, 30 (2016) https://doi.org/10.3390/ijms17010030

9. Galicia-Moreno Marina, Jorge A Silva-Gomez, et al. Liver Cancer: Therapeutic Challenges and the Importance of Experimental Models. Canadian Journal of Gastroenterology and Hepatology, 1,10 (2021) https://doi.org/10.1155/2021/8837811
10. Raj Priyadarsini, Samuel Abiseik, Kothandapani Anitha. Computational quest, synthesis and anticancer profiling of 3-methyl quinoxaline-2-one-based active hits against the tyrosine kinase. Future Journal of Pharmaceutical Sciences, 10, 137 (2024) https://doi.org/10.1186/s43094-024-00711-4
11. Wenping Wang, XiaoXv Dong, et al. Itraconazole exerts anti-liver cancer potential through the Wnt, PI3K/AKT/ mTOR, and ROS pathways. Biomedicine & Pharmacotherapy, 131, 110661 (2020) https://doi.org/10.1016/j.biopha.2020.110661
12. Yan-jing ZHU, Bo ZHENG1, et al. New knowledge of the mechanisms of sorafenib resistance in liver cancer. Acta Pharmacologica Sinica, 38, 614–622 (2017) https://doi.org/10.1038/aps.2017.5
13. Yadav Nalini, Kumar Parveen, et al. Development of 1,3,4-oxadiazole thione based novel anticancer agents: Design, synthesis and in-vitro studies. Biomedicine & Pharmacotherapy, 95, 721–730 (2017) http://dx.doi.org/10.1016/j.biopha.2017.08.110
14. Rao Vijaya Pidugu, Sastry Nagendra Yarla, et al. Design and synthesis of novel HDAC8 inhibitory 2,5-disubstituted-1,3,4-oxadiazoles containing glycine and alanine hybrids with anticancer activity. Bioorganic & Medicinal Chemistry, 24, 5611–5617 (2016) http://dx.doi.org/10.1016/j.bmc.2016.09.022
15. Puttaswamy Naveen, Malojiao Vikas H., et al. Synthesis and amelioration of inflammatory paw edema by novel benzophenone appended oxadiazole derivatives by exhibiting cyclooxygenase-2 antagonist activity. Biomedicine & Pharmacotherapy, 103, 1446–1455 (2018) https://doi.org/10.1016/j.biopha.2018.04.167
16. Philip John Ameji, Adamu Uzairu, et al. Computer aided design of novel antibiotic drug candidate against multidrug resistant strains of *Salmonella typhi* from pyridine-substituted coumarins. Beni-Suef Univ J Basic Appl Sci, 13, 15(2024) https://doi.org/10.1186/s43088-024-00473-1
17. Araújo de Brito Monique. Pharmacokinetic study with computational tools in the medicinal chemistry course. Brazilian Journal of Pharmaceutical Sciences, 47, 797 (2011) https://doi.org/10.1590/S1984-82502011000400017
18. Deshmukh Nitin, Soni Love Kumar. Prediction of In-silico ADMET Properties and Molecular docking study of Substituted Thiadiazole for screening of Antiviral activity against protein target

Covid-19 main protease. Research J. Pharm. and Tech, 16(12), 5802-5807 (2023) https://doi.org/10.52711/0974-360X.2023.00939

19. Kuchana Madhavi, Kambala Lakshmi. Design, synthesis and *in silico* prediction of drug-likeness properties of new *ortho*, *meta* and *para*-(2-cyano-3-(3,5-di-*tert*-butyl-4-hydroxyphenyl)acrylamido)benzoic acids. Journal of Applied Pharmaceutical Science, 11(08), 031-035 (2021) https://doi.org/10.7324/JAPS.2021.110805
20. Sundara Prabha. V, Ajitha. I, Beschi Antony Rayan. In Silico Analysis of Selected Compounds Using Pass, Swissadme and Molinspiration. IJSDR, 7, 542-546 (2022)
21. Deshmukd Nitin, Soni Love Kumar. Prediction of *in silico* ADMET Properties and Molecular Docking Study of Substituted Thiadiazole for Screening of Antibacterial and Antifungal Activities against Protein Targets Helicobacter pylori ⟨-Carbonic Anhydrase and *Trypanosoma brucei* Pteridine Reductase. Asian Journal of Organic & Medicinal Chemistry, 7, 65–74 (2022) https://doi.org/10.14233/ajomc.2022.AJOMC-P363
22. Mishra Shashank Shekhar, Sharma Chandra Shekhar. In silico ADME, Bioactivity and Toxicity Parameters Calculation of Some Selected Anti-Tubercular Drugs. eIJPPR, 6(6), 77-79 (2016) https://doi.org/10.24896/eijppr.2016661
23. Ragab Fatma, Abou-Seri Sahar. Design, synthesis and anticancer activity of new monastrol analogues bearing 1,3,4-oxadiazole moiety. European Journal of Medicinal Chemistry, 17, 30472-510 (2017) doi: https://doi.org/1016/j.ejmech.2017.06.026
24. Stamos Jennifer, Sliwkowski Mark, Eigenbrot Charles. Structure of the Epidermal Growth Factor Receptor Kinase Domain Alone and in Complex with a 4-Anilinoquinazoline Inhibitor. The journal of biological chemistry, 277: 46265–46272 (2002) https://doi.org/10.1074/jbc.M207135200